Siderophore Analogues. Synthesis and Chelating Properties of a New Macrocyclic Trishydroxamate Ligand

M. Alexandra Esteves,[a] M. Cândida T. Vaz,[a] M. L. S. Simões Gonçalves,[a] Etelka Farkas[b] and M. Amélia Santos*[,a]

[a] *Centro de Química Estrutural, Complexo I, Instituto Superior Técnico, 1096 Lisbon codex, Portugal*

[b] *Department of Inorganic and Analytical Chemistry, University of Debrecen, H-4010 Debrecen, Hungary*

A new iron(III)-specific ligand, 1,5,9-triazacyclododecane-*N*,*N*',*N*''-tris(*N*-methylacetohydroxamic acid) H_3L, containing three hydroxamic acid groups as pendant arms on a macrocyclic triamine backbone, has been synthesized and characterized. Its acid–base and chelating properties with iron(III) and copper(II) ions have been studied by potentiometric and spectrophotometric techniques. The mechanism of electron transfer as well as the kinetics of dissociation and stability constants of reduced species, which are thought to be important in the biological activity of this siderophore analogue, have been studied by voltammetric methods. This ligand has proved to be biologically active and its properties were compared with ferrichrome and ferrioxamine B.

Iron is essential for the growth of all cells. To circumvent the iron(III) insolubility problem under physiological conditions, adequate uptake of iron(III) from the environment into microbial cells is carried out by certain low-molecular weight chelating agents, called siderophores, which are produced by microorganisms.[1] The high affinity of siderophores (or synthetic models) for iron makes them useful as drugs to facilitate iron mobilization in humans, especially in the treatment of iron diseases.[2] Siderophores, in the main, employ catecholate and hydroxamate ligands for chelating to iron(III); however, some dihydroxamate siderophores are also known such as the naturally occurring rhodotorulic acid.[3]

The naturally occurring hydroxamate-type siderophores, including ferrichrome, rhodotorulic acid, coprogen, aerobactin, vary considerably with respect to the placement of the hydroxamate groups in different molecular backbones. However all of them have in common the fact that the hydroxamate groups are bridged by amide-containing methylene chains, whose function is not yet clarified, but has been related to siderophore recognition by outer-membrane receptor proteins.[2]

Synthetic iron-sequestering agents are of current interest and various attempts have been made to develop effective siderophore analogues for biomedical or analytical purposes.[4–8] Also in this context there have been an increasing number of publications on aminohydroxamic acids, and their metal complex-forming ability.[9–12]

We have recently reported two cyclic diaminodihydroxamic acids,[13,14] as analogues of rhodotorulic acid, which showed some biological activity. We therefore felt encouraged to attempt to improve the biological performance of this type of ligand by further modification. First, we aimed to improve the iron binding efficiency, by providing the cyclic amine backbone with an extra hydroxamate group, to enable the iron to be fully co-ordinated by the ligand, thus simulating ferrichrome. Upon undertaking a molecular-modelling study[15] we decided to synthesize a new macrocyclic triazatrihydroxamate ligand 1,5,9-triazacyclododecane-*N*,*N*',*N*''-tris(*N*-methylacetohydroxamic acid) H_3L, Fig. 1. This ligand contains a triaza macrocyclic ring, 1,5,9-triazacyclododecane [12]aneN_3, as a basic building block whose conformation appeared suitable to enable the trifunctional hydroxamate moieties to be well oriented to co-ordinate to the iron(III) centre. The backbone cyclic amine, having high basicity, endows a zwitterionic character to the ligand, and is a factor in the good water solubility of both the ligand and its iron(III) complex. This

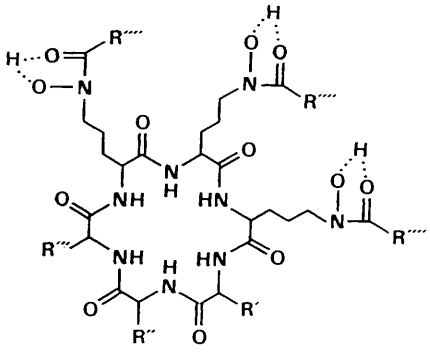

Desferriferrichrome

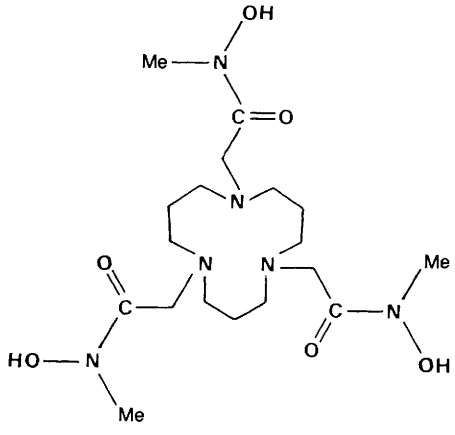

H_3L

Fig. 1 Structural formulae for desferriferrichrome and the synthetic trishydroxamate ligand

feature deserves particular attention due to the potential utilization of this new ligand as a drug. Also, the fact that this ligand contains both lipophilic and hydrophilic moieties is expected greatly to facilitate the transport process through membranes. This ligand resembles in some way the trihydroxamate siderophore desferriferrioxamine-B which also

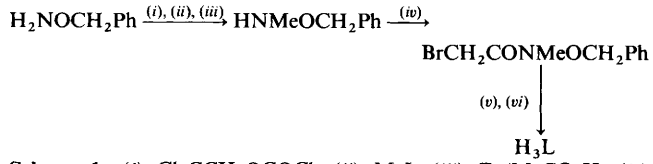

Scheme 1 (*i*) Cl_3CCH_2OCOCl; (*ii*) MeI; (*iii*) $Zn/MeCO_2H$; (*iv*) $BrCH_2COBr$; (*v*) [12]$aneN_3$; (*vi*) H_2–Pd/C

contains a terminal amine group, and has been used for the treatment of iron overload diseases such as Cooley's anaemia.

The ligand H_3L is biologically active in various bacteria, even those containing ferrichrome receptors.[16] This siderophore analogue does not contain amide groups, which are thought to be important for siderophore recognition by cellular membrane receptor proteins. Since simple hydroxamic acids usually do not show such biological activity it is anticipated that the amino groups in the macrocyclic ring might play an important role in the biological properties, mimicking to some extent the function attributed to amide groups in the naturally occurring siderophores.

In this paper we report on the preparation of the new siderophore analogue, as well as a study of its acid–base and complexing properties, not only with iron but also with copper, both for comparative purposes as well as the fact that copper is an essential trace element which plays an important role in many biological systems. The electron-transfer properties of the metal chelates are analysed in detail, taking into account that changes in valence state of the Fe^{III} centre have been postulated in the transport mechanism of some siderophores, *e.g.* with ferrichrome in *Escherichia coli*.[1,17] In the absence of X-ray data, molecular-mechanics calculations are employed to provide information about the possible molecular structure of the iron(III) in its complex [FeL], the theoretical lowest energy conformer.

Results and Discussion

Synthesis.—Structurally, this new ligand is composed of a triazamacrocyclic ring as a backbone with three N-attached side chains, each containing a bidentate hydroxamate group. While the hydroxamate groups are in a reversed direction relative to that of ferrichrome (see Fig. 1), this difference is not considered important in terms of biological properties.[18] Although the macrocyclic amine [12]$aneN_3$ is commercially available, its synthesis being also well described in the literature,[19,20] the hydroxamate group is chemically very delicate so making the overall synthesis of H_3L more challenging.

Although in similar ligands[13,14] the preparation of two *N*,*N*-dihydroxamate derivatives of cyclic diamines had been previously possible by direct coupling of the α-halogenoacetohydroxamic acid with the corresponding cyclic amine, this process was not successful in preparing the [12]$aneN_3$ trihydroxamate derivative. This differing behaviour is attributed to the considerable sensitivity of the hydroxamate group to hydrolysis, namely associated with the requirement for use of more basic reaction conditions. This problem led us to look for a hydroxamate protecting group which should remain inert during *N*-functionalization of the macrocycle, but which could be subsequently easily removed. After unsuccessful results with *O*-acetyl[21] we found *O*-benzylic protection, also previously described,[22] to be successful. The overall synthesis of H_3L can be summarized in three main steps, according to Scheme 1: (*i*) preparation of the *N*-methyl-*O*-benzylhydroxylamine by methylation of *O*-benzylhydroxylamine, involving intermediate Cl_3CCH_2OCO protection and deprotection; (*ii*) preparation of the *O*-protected hydroxamic acid *O*-benzyl-2-bromo-*N*-methylacetohydroxamic acid, by *N*-acylation of the corresponding hydroxylamine; and (*iii*) coupling between the nitrogen atoms of the macrocyclic amine, [12]$aneN_3$, and the acetyl α-carbon atoms of the *O*-protected hydroxamic acid, followed by *O*-deprotection, leading to the ligand H_3L.

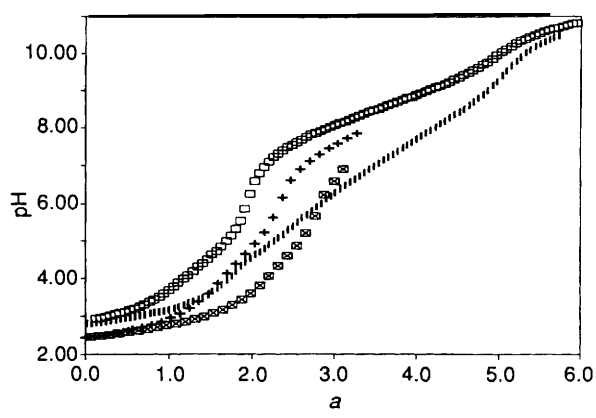

Fig. 2 Potentiometric titration curves (experimental points) for the ligand H_3L (□), copper(II)–H_3L system (II), $c_L/c_{Cu} = 1:1$, $c_L = 1.3 \times 10^{-3}$ mol dm^{-3} and iron(III)–H_3L system, $c_L/c_{Fe} = 5:1$, $c_L = 2.3 \times 10^{-3}$ mol dm^{-3} (+); $c_L/c_{Fe} = 10:1$, $c_L = 3.1 \times 10^{-3}$ mol dm^{-3} (⊠); *a* = moles of base added per mol of ligand present

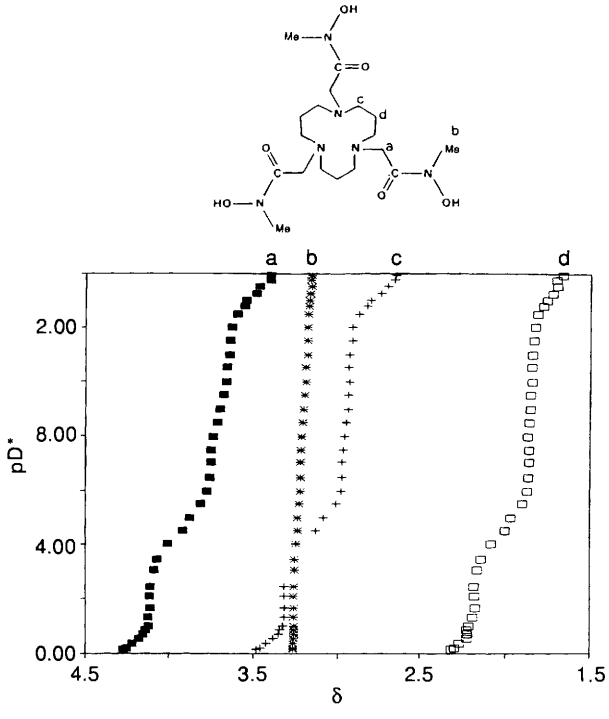

Fig. 3 Proton NMR titration curves for H_3L, using KOD as titrant (δ as a function of pD*)

Protonation Properties.—Ligand H_3L in its completely deprotonated form, L^{3-}, has six basic sites that can be protonated: three amine groups in the macrocyclic ring and three hydroxamate groups. The protonation constants were determined by potentiometric titration of the fully protonated ligand with sodium hydroxide (Fig. 2). However, this technique only allowed the accurate determination of four protonation constants, *viz.*: $\log K_2 = 9.20 \pm 0.01$, $\log K_3 = 8.52 \pm 0.01$, $\log K_4 = 7.68 \pm 0.01$, $\log K_5 \pm 4.69 \pm 0.01$ ($K_n = [H_nL]/[H_{n-1}L][H^+]$). The first and sixth protonation constants were too high and too low, respectively, to be accurately determined by direct potentiometry, since under our experimental conditions this method is limited to the range pH 2–12.[23] Therefore both the remaining K_n values were only roughly estimated from the ^1H NMR titration curves

Table 1 Protonation constants of H_3L, [12]aneN$_3$, H_3L' (25.0 ± 0.1 °C, I = 0.1 mol dm^{-3}), desferriferrioxamine B and desferriferrichrome

	H_3L[a]	[12]aneN$_3$[b]	H_3L'[c]	Desferriferrioxamine[d]	Desferriferrichrome[d]
log K_1	> 12	12.6	12.8	10.40	9.83
log K_2	9.20	7.57	7.55	9.70	9.00
log K_3	8.52	2.41	3.65	9.03	8.11
log K_4	7.68	—	2.1	8.39	—
log K_5	4.69	—	—	—	—
log K_6	< 2	—	—	—	—

[a] This work. [b] From ref. 25. [c] From ref. 26. [d] From ref. 27.

illustrated in Fig. 3. These curves result from the fact that protonation of basic groups increases their deshielding effect and resonances of the methylene protons are shifted downfield. Such chemical shift (δ) pH dependence, which is significant for methylene protons near to certain basic sites, such as amine groups,[24] enabled us roughly to estimate log K_n (n = 1 or 6) and to locate the sites of protonation. Protonation constants of H_3L are given in Table 1, together with the corresponding values for similar ligands, for comparison.

Analysis of the set of data presented in Table 1 and the ^{1}H NMR titration curves indicates that for L^{3-} the first protonation process (log K_1 > 12) occurs at one of the macrocyclic nitrogens, similarly to that observed for other ligands containing the same macrocyclic backbone, such as [12]aneN$_3$[25] and the corresponding triacetic acid derivative (H_3L').[26] In fact for all such compounds the first protonation constant is high owing to the formation of a hydrogen bonding network where, due to conformational preferences, the three nitrogen atoms are linked in pairs by three-atom bridges,[28] structure **I**.

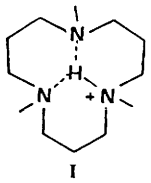

I

According to ^{1}H NMR titration curves and also to the range of values known for hydroxamate protonation constants (log K = 8–9),[29] the values measured for log K_2, log K_3 and log K_4 are attributed to protonation of the side-chain hydroxamate moieties. The difference between these three log K_n values determined for H_nL indicates essentially statistical behaviour[23] and so they are quite independent from each other in the protonation process. Furthermore, these values compare well with the corresponding values for some trihydroxamate siderophores presented in Table 1, such as desferriferrioxamine B (8.39–9.70) and desferriferrichrome (8.11–9.38).[27]

From Fig. 3 it can be seen that the chemical shifts of propylene protons of the macrocyclic ring (**c**, **d**) and hydroxamate methylene protons (**a**) change considerably and similarly over the pD* intervals 12–13.5, 3–6 and 0–2 (pK_D = 0.11 + 1.10 pK_H).[30] This suggests that, in addition to the first protonation constant, the fifth and sixth protonations are at ring-amine groups. The very low value estimated for the last protonation constant (log K_6 < 2), similarly found in other cyclic amines such as in other [12]aneN$_3$ derivatives, is ascribed to high coulombic repulsive forces resulting from the existence of three protonated amine groups close to each other in the ring. The fifth constant (log K_5 = 4.69), corresponding to a protonation of the second ring-amine groups, is lower than those found for the corresponding process in [12]aneN$_3$ and its triacetic acid derivative (log K_2 = 7.5–7.6). This difference is due to the fact that while in the latter two derivatives the second N-protonation process is governed by coulombic effects, in H_3L we have to consider the effect of the presence of side arms

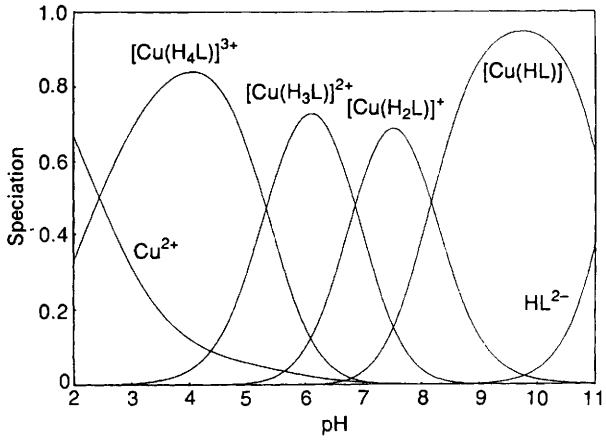

Fig. 4 Speciation curves for the Cu^{II}–H_3L system as a function of pH (c_L/c_{Cu} = 1:1, c_L = 1.3 × 10^{-3} mol dm^{-3})

(hydroxamate moieties) that are more basic than both the remaining unprotonated ring-amines. Therefore the protonation of this second ring-amine centre is inhibited by hydrogen-bond interactions between the hydroxamate protons and the unprotonated amines through a six-membered ring intermediate **II**.

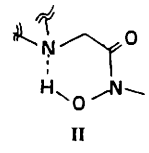

II

Copper–H_3L System.—The affinity of H_3L in copper(II) complexation was studied by potentiometry using the SUPERQUAD program upon data obtained from three titration curves at different metal to ligand ratios (1:1, 1:2, 2:1) and c_L = 1.3 × 10^{-3} mol dm^{-3}. The copper(II)–ligand (1:1) titration curve is shown in Fig. 2. No insoluble species were observed in the range pH 2–11 and complex formation occurred even at very low pH, thus involving protonated species. The model was fitted with four copper(II) complex species $[Cu(H_4L)]^{3+}$, $[Cu(H_3L)]^{2+}$, $[Cu(H_2L)]^+$ and [Cu(HL)] with log β of 31.81 ± 0.02, 26.88 ± 0.02, 19.95 ± 0.02 and 11.95 ± 0.02 respectively {$\beta_{Cu(H_nL)}$ = [Cu(H_nL)]/[Cu][H]^n[L]}.

Structural attributions to these complexes are difficult because H_3L can adopt a variety of chelating modes *e.g.* O,O (hydroxamate, hydroxamate) or O,N (hydroxamate, macrocyclic amine).

The species distribution of the copper(II) complexes with H_3L at a 1:1 metal-to-ligand molar ratio, as a function of pH, is shown in Fig. 4. The existence of protonated copper complexes in neutral or even basic conditions indicates only minor involvement of amino groups in co-ordination. In order to obtain an insight into the nature of co-ordination involved in these copper(II)–H_3L complexes, the absorbance spectra of aqueous solutions were recorded as a function of pH (c_L : c_{Cu} =

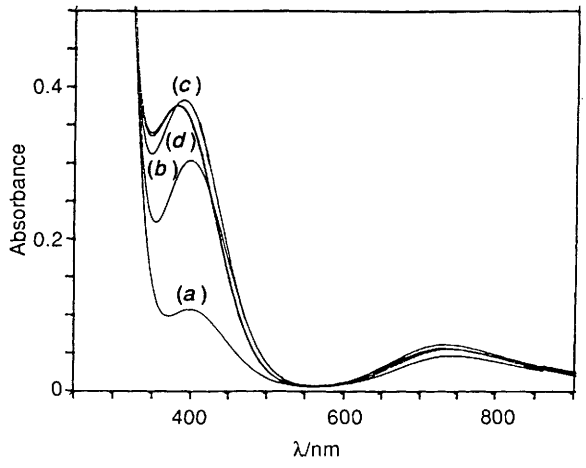

Fig. 5 Absorbance spetra of Cu^{II}–H_3L complexes as a function of pH (c_L/c_{Cu} = 4:1, c_{Cu} = 4.5 × 10^{-4} mol dm^{-3}); pH 5.3 (*a*), 6.5 (*b*), 7.9 (*c*) 9.2 and 10.5 (*d*)

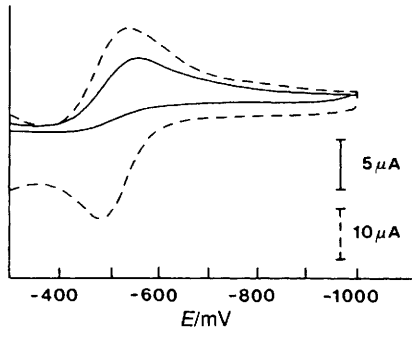

Fig. 6 Cyclic voltammograms for the Cu–H_3L system at pH 7.0 and different scan rates, v = 100 (——) or 5000 (– – –) mV s^{-1}; c_L/c_{Cu} = 20:1, c_{Cu} = 2.5 × 10^{-4} mol dm^{-3}

4:1; c_{Cu} = 4.5 × 10^{-4} mol dm^{-3}) and are shown in Fig. 5. Aqueous solutions are pale green in the pH range 5.3–10.4. Absorption spectra at different pH values show two bands, one at λ_{max} = 750 nm (ε_{max} = 138 dm^3 mol^{-1} cm^{-1}; pH 7.9) the other at λ_{max} = 390 nm (ε_{max} = 851 dm^3 mol^{-1} cm^{-1}; pH 7.9). These bands are characteristic of hydroxamic oxygen binding to Cu^{II}, as suggested by similar results for copper(II)–dihydroxamic acid complexes,[31] and have been assigned to d–d and charge-transfer (c.t.) transitions, respectively. Therefore, although other types of co-ordination could be considered, taking into account the ability of copper(II) to co-ordinate with *N*- and *O*-donors, analysis of spectrophotometric data, together with the protonation results strongly supports predominance of hydroxamate co-ordination, at least in the range pH 5.3–9. Observed increases in absorbances and small shifts to shorter wavelengths with increasing pH (up to pH 7.9) suggest an increased degree of co-ordination to hydroxamate groups. At pH > 9 a decrease in the absorption intensity of the c.t. band may correspond to a change in co-ordination, probably involving a competing hydroxide group co-ordination.

Summarizing, these results together with the protonation studies suggest that all characterized copper(II)–H_3L complexes contain the ligand with the triaza ring in a monoprotonated form with preferential co-ordination of the metal ion to the hydroxamate groups. This may be attributed to the higher basicity of the hydroxamate groups relative to both the remaining unprotonated amine groups. Since Cu^{2+} often adopts a co-ordination number of four in this type of complex,[9] in the [Cu(HL)] species one of the hydroxamate groups will be unco-ordinated and is protonated below pH 8 to give $[Cu(H_2L)]^+$. For $[Cu(H_3L)]^{2+}$ the third proton could reside on either an amine or a hydroxamate group, while under more acidic conditions (pH 2.5–5) where $[Cu(H_4L)]^{3+}$ predominates two macrocyclic amine N atoms and two hydroxamate groups are probably protonated. The likely non-co-ordination of the metal to the amine group (due to the ready protonation of the cyclic amine and resulting hydrogen bonding) is also supported by the fact that the parent cyclic amine ligand [12]aneN_3 is unable to form a copper(II) complex species in any protonated form.[26]

Electrochemical studies for the Cu^{2+}–H_3L system were carried out by cyclic voltammetry in aqueous solution. Although a cathodic peak with its anodic counterpart (see Fig. 6) was observed, this system does not display simple redox behaviour and a detailed analysis is therefore required. The ratio $i_p^c/v^{\frac{1}{2}}$ decreases with increasing scan rate v. The cathodic peak, which shows a larger width at lower scan rates, probably results from the overlapping of two peaks attributed to differing copper species: one due to reduction of dissociated copper complex O′ (Scheme 3) and the other to direct reduction of the complex O (Scheme 2). The peak separation, ΔE_p decreases from *ca.* 100 mV at v = 200 mV s^{-1} to *ca.* 60 mV at v ≈ 10 000 mV s^{-1}. These results suggest, for higher scan rates, a reversible electrochemical behaviour with exchange of one electron, probably due to the reduction–oxidation of the complex (O/R) directly at the electrode (Scheme 2). Reduction of copper(I) to copper(0) cannot be detected due to overlap of reduction of the proton.

$$\text{Reduction: } O + e \rightleftharpoons R \quad (1)$$

$$\text{Oxidation: } R \rightleftharpoons O + e \quad (2)$$

Scheme 2 Redox behaviour of the Cu–H_3L system in the high scan rate range

At lower scan rates chemical reactions (C) occur in conjunction with electrochemical processes (E) and a CEC mechanism operates (Scheme 3) involving the predissociation of the copper(II) complex [equation (3)] followed by reduction

Reduction:

$$O \rightleftharpoons O' \text{ (C)} \quad (3)$$

$$O' + e \rightleftharpoons R' \text{ (E)} \quad (4)$$

$$R' \rightleftharpoons R \text{ (C)} \quad (5)$$

Oxidation:

$$R \longrightarrow R'' \text{ (C)} \quad (6)$$

$$R \rightleftharpoons R' \text{ (C)} \quad (7)$$

$$R' \rightleftharpoons O' + e \text{ (E)} \quad (8)$$

$$O' \rightleftharpoons O \text{ (C)} \quad (9)$$

Scheme 3 Redox behaviour of the Cu–H_3L system in the low scan rate range

of the dissociated Cu^{II} ion O′ [equation (4)] and complex formation by the reduced copper(I) species [equation (5)] since Cu^{I} is unstable when uncomplexed. In the oxidation process, under the same conditions, we must have a global CCEC mechanism [equations (6)–(9)] which includes a term relating to irreversible decomposition of the reduced copper complex to R″ [equation (6)] together with the reverse processes relative to the reduction mechanism, *i.e.* dissociation of the copper(I) complex [equation (7)] followed by oxidation of the dissociated copper(I) species R′ [equation (8)], and finally complex formation [equation (9)]. That the chemical decomposition step (R ⟶ R″) occurs is supported by a decrease of the $i_p^c : i_p^a$ ratio from *ca.* 3 to 1 : 1 for scan rates between 200 and 5000 mV s^{-1} (at higher scan rates adsorption effects are found).

For intermediate scan rates both the mechanisms of Schemes 2 and 3 occur, leading to overlapping of the corresponding peaks.

The irreversible chemical decomposition of the copper(I) complex probably results from a change of co-ordination mode and conformation upon reduction, this process being slow on the time-scale of the experiment. While Cu^{II} readily co-ordinates to the oxygen atoms of the hydroxamate 'arms', the

'softer' character of Cu^{I} ion makes this co-ordination less favourable and probably leads to preferential partial co-ordination to the nitrogen atoms of the ring. However, co-ordination involving only the nitrogen atoms of the ring does not seem probable owing to the high basicity of the amine ring. Also, from the invariant values of E_p^c and E_p^a obtained for different ligand concentration (ratios $c_L:c_M$ between 10 and 30:1), the same co-ordination number with respect to the ligand is suggested for both oxidized and reduced species.[32a]

Therefore, for scan rates in the range 2000–5000 mV s^{-1}, Cu^{II} is probably reduced to Cu^{I}, both in complexed form, and without adsorption. Furthermore values of E_p^c show a cathodic shift with pH [$(\Delta E/\Delta(pH) \approx 49$ mV)] in the range 10 > pH > 6 (see Fig. 7), thus suggesting involvement of one electron and one proton in the redox process.

Taking into account the potentiometric results and assuming that we have the same type of complex, a speciation study, under the experimental conditions used for the cyclic voltammetric measurements, gives the dominant oxidized species at pH 7.0 as $[Cu(H_2L)]^+$ (≈44%) and $[Cu(H_3L)]^{2+}$ (≈54%). If we assume that at v = 2000 mV s^{-1} the electrochemical process is practically reversible and both chemical processes can be neglected, the stability constant for the reduced species at 25 °C can be estimated from the DeFord and Hume equation[32b] considering that the copper(II) complexes are $[Cu(H_nL)]^{n-1}$ ($n = 2$ or 3) and that the copper(I) species is mainly $[Cu(H_3L)]^+$.

For this specific case equation (10) holds where $K_H^{II} =$

$$E_p^c - E_p^s = -59.15\left[\log \frac{1 + K_H^{II}[H^+]}{[H^+]} + \log \frac{\beta^{II}_{Cu(H_2L)}}{\beta^{I}_{Cu(H_3L)}}\right] \quad (10)$$

$[Cu(H_3L)]/\{[Cu(H_2L)][H^+]\} = 10^{6.85}$ dm^3 mol^{-1} and β values are the global formation constants. From equation (10) it can be seen that a shift of E_p^c should happen for values of pH > 6 that should tend to zero for smaller pH values.

Using $E_p^s = -134$ mV, as previously defined,[14] $E_p^c = -550$ mV and the β value of the copper(II) complex obtained from potentiometry, corrected for the ionic strength ($I = 1$ mol dm^{-3}, KNO_3), we calculated the global formation constant for the reduced copper complex, $\log \beta^{I}_{Cu(H_3L)} = 18.75$.

The rate constant of the slow decomposition of $[Cu^{I}(H_3L)]^+$ was calculated according to the Nicholson and Shain approach,[33] as previously described.[14] The calculated value, $k_d = 1.9 \pm 0.1$ s^{-1} was obtained as an average of several single-point calculations (see Table 2), corresponding to different scan rates in the range 600–1000 mV s^{-1}, where adsorption effects are neglected.

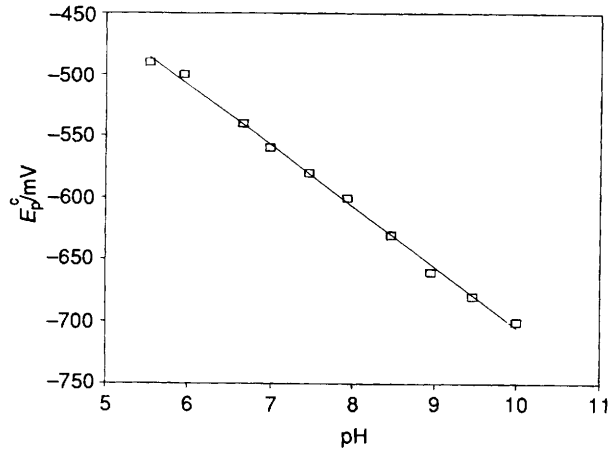

Fig. 7 Cathodic shift of E_p^c with pH, observed in the voltammograms of the Cu–H_3L system, at a scan rate v of 200 mV s^{-1}; $c_L/c_{Cu} = 20:1$, $c_{Cu} = 2.5 \times 10^{-4}$ mol dm^{-3}

Comparison of the reduction peak potential obtained for the copper(II)–copper(I) system in the presence of our ligand ($E_p^c = -0.55$ V at v = 0.2 V s^{-1}), with that obtained in the presence of a tetraazamacrocyclic ligand, 1,4,8,11-tetraazacyclotetradecane ([14]aneN$_4$) ($E_p^c = -0.94$ V at v = 0.2 V s^{-1}),[34] may also give support to the existence of a different metal co-ordination to HL_3, namely with a major participation of hydroxamate groups, instead of amine groups, as in [14]aneN$_4$.

Iron–H_3L *System*.—Stability constants for iron(III)–H_3L complexes were determined by spectrophotometric titrations. This ligand reacts with Fe^{III} over a wide pH range (2–10), as indicated by the absorption spectra (Fig. 8). The complexes were generated *in situ* by addition of a standard iron(III) nitrate solution to the ligand, present in ten-fold excess to prevent potential precipitation of iron(III) hydroxides. In the range 5 < pH < 9, a band centred at 425 nm is observed with ε_{max} *ca.* 3000 dm^3 mol^{-1} cm^{-1} (Fig. 9). According to previous studies,[6,13] such spectra can be ascribed to a complex in which three hydroxamate moieties are co-ordinated to one iron(III) centre. Since our ligand has three hydroxamate groups and one protonated ring-amine under our experimental conditions, we assume that under these conditions a 1:1 (iron:ligand) complex

Table 2 Scan rate effect on the i_p^a/i_p^c ratio and calculated kinetic parameters for the copper(I)–H_3L system at pH 7; $c_L:c_{Cu} = 20:1$, $c_{Cu} = 2.5 \times 10^{-4}$ mol dm^{-3}

v/mV s^{-1}	i_p^a/i_p^c	$k_d\tau$	$E_{\frac{1}{2}}$/mV	τ*/s	k_d/s^{-1}
600	0.42	1.52	−515	0.81	1.88
700	0.43	1.44	−510	0.70	2.06
800	0.46	1.21	−515	0.61	1.98
900	0.48	1.08	−515	0.54	2.00
1000	0.49	1.03	−515	0.49	2.10
2000	0.72	0.36	−510	0.24	1.50

* $\tau = (E_{\frac{1}{2}} - E_\lambda)/v$, with $E_\lambda = -1000$ mV.

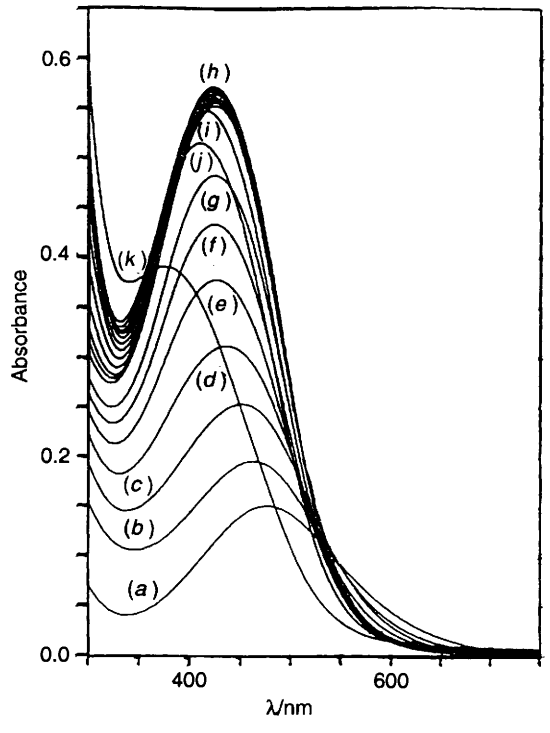

Fig. 8 Absorbance spectra of the Fe^{III}–H_3L system in aqueous solution as a function of pH; $c_L/c_{Fe} = 10:1$, $c_{Fe} = 1.8 \times 10^{-4}$ mol dm^{-3}. Equilibrium pH values: 1.96 (*a*), 2.46 (*b*), 2.97 (*c*), 3.46 (*d*), 4.09 (*e*), 4.64 (*f*), 5.00 (*g*), 5.5–10.0 (*h*), 10.50 (*i*), 10.94 (*j*), 11.43 (*k*)

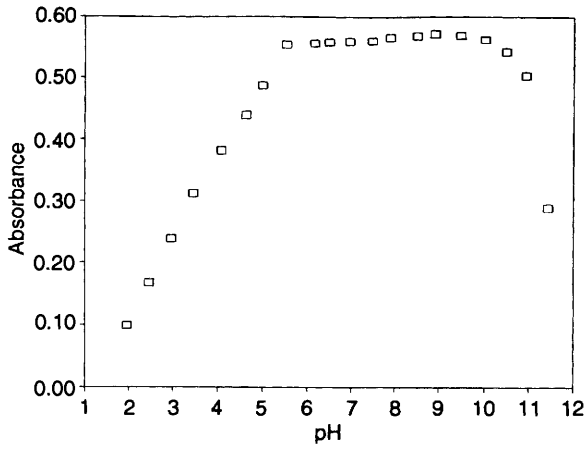

Fig. 9 Variation of the absorbance of Fe^{III}–H_3L solution as a function of pH at λ_{max} = 425 nm; c_L/c_{Fe} = 10:1, c_{Fe} = 1.8 × 10^{-4} mol dm^{-3}

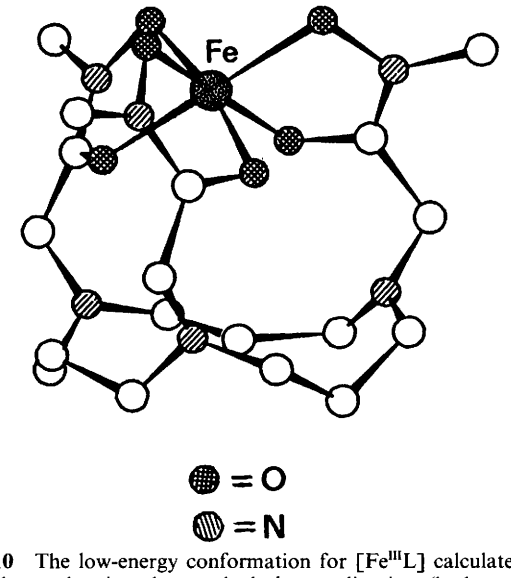

Fig. 10 The low-energy conformation for $[Fe^{III}L]$ calculated in the gas phase, showing the octahedral co-ordination (hydrogen atoms are omitted)

$[Fe(HL)]^+$ is the major species, if indeed the only one, at measurable concentrations. Decreasing pH (to 2) leads to a decrease in the band intensity which, at pH < 4, is accompanied by a decrease in energy (bathochromic shift). This may indicate a decreasing number of hydroxamate moieties co-ordinated to the metal centre, due to stepwise dissociation from the complex, with probable concomitant formation of colourless hexaaquairon species. On the other hand, above pH 9 a hypsochromic shift is observed which is probably due to hydroxide competing with hydroxamate in co-ordination to iron(III).

No single isosbestic point encompassing all the spectra in the pH range 2–10 is observed, which indicates that more than two iron(III) species exist in solution in the pH range. Changes in the visible spectrum allow the spectrophotometric determination of stepwise formation constants. In the pH range 3–9 only two relevant species $[Fe(HL)]^+$ and $[Fe(H_2L)]^{2+}$ were obtained in best-fitting models for the interpretation of spectrophotometric titration data of this binary system. Refined global stability constants were obtained with the PSEQUAD program [log $\beta_{Fe(HL)}$ = 24.18 ± 0.06, log $\beta_{Fe(H_2L)}$ = 27.45 ± 0.02]. The stability constant calculated for $[Fe(HL)]^+$ is lower than that calculated for ferrichrome (log β = 29.1) or monoprotonated ferrioxamine B (log β = 30.5).[27] This difference may be due to some stereochemical strain in $[Fe(HL)]^+$, resulting from the fact that it contains shorter hydroxamate chains than ferrichrome or even to an electrostatic effect due to the proximity of the Fe binding centre to the macrocyclic ring proton in HL^{2-}. This effect is less important in the amino-protonated ferrioxamine B because the ammonium terminal proton is separated from the hydroxamate group by a longer alkyl chain (five methylene groups instead of one, as in HL^{2-}).

Potentiometric studies on this binary system were also carried out (Fig. 2) giving formation constant values in close agreement to the above. However, taking into account the limiting experimental conditions, such as the small range of pH (2 < pH < 7) investigated, the large excess of ligand required, and the lack of competition between protons and iron(III) in such a strong complex involving trihydroxamic acid ligands, the measured stability constant was subject to large errors. In this context stability constants determined by spectrophotometry are more reliable because the $[Fe(HL)]^+$ species is directly observed. Moreover, at pH 8 the formation constant for the dominant species {the $[Fe(HL)]^+$ complex} was confirmed by spectrophotometric competition studies with ethylenediamine-*N*,*N*,*N*′,*N*′-tetraacetate (edta). Although other species are present, their presence is only significant under more acid or basic conditions than those used in the calculations.

Therefore in the pH range 5–9 the $[Fe(HL)]^+$ complex predominates. From the pH dependence of the spectra (Fig. 3), a lower degree of co-ordination to iron(III) by hydroxamate moieties in $[Fe(H_2L)]^{2+}$ can be inferred. Therefore it appears that the preferential site for the second protonation of the complex should be at hydroxamate rather than at an amine-ring group. This is consistent with the above discussed basicity of the macrocyclic triamine ring and consequently the increased difficulty of further protonation.

In order to obtain an insight into the probable structure of [FeL] in the absence of suitable crystals for X-ray diffraction, preliminary molecular-mechanics studies were carried out using the CERIUS software package.[35] The universal force field (UFF)[36] was used, with the exception of terms related to iron(III) co-ordination. To find the best set of parameters for the metal and chelate moieties we interactively fitted a model structure of a iron(III)–trisbenzohydroxamate complex to its known experimental crystal structure.[15] Using these optimized parameters the unprotonated [FeL] complex was then modelled by molecular-mechanics methods and the minimized structure is shown in Fig. 10. The ligand seems to adopt a structure with *N*-ring atoms in a macrocyclic mean plane, and hydroxamate arms axially directed out of this plane in a concerted direction, leading to octahedral co-ordination to the iron(III) centre above this plane [Fe···N (av.) 4.15 Å]. The monoprotonated complex $[Fe(HL)]^+$ should have a similar structure, this having the amine and protonated amine groups as available sites for potential membrane protein recognition, such as is the case with ferrichrome amide groups. Further work on the preparation of crystals suitable for X-ray structure determination is in progress.

Electrochemistry of the Fe–H_3L system was studied by cyclic voltammetry at neutral pH in aqueous solution. The reduction waves observed for $[Fe(HL)]^+$ (see Fig. 11) are consistent with a quasi-reversible system with $E_{\frac{1}{2}}$ = −530 mV. The magnitude of the Fe^{III}–Fe^{II} reduction potential in this system (E_p^c = −630 mV) is in the range found for physiological reductants, such as NADH (reduced nicotinamide-adenine dinucleotide).[37] Indeed, this redox process seems to be slightly easier than for the natural siderophores ferrichrome and ferrioxamine B which have $E_{\frac{1}{2}}$ values of −0.69 and −0.698 V, respectively (*vs.* SCE, 1 mol dm^{-3} KCl supporting electrolyte).[38] At an L:Fe ratio of 20:1, cyclic voltammograms exhibit a peak separation of approximately 180–200 mV at pH 7. According to Nicholson and Shain[33] it is possible to obtain the transfer coefficient, α, by plotting log *i* *vs.* $(E - E_i)$, for $i < 10\%$ i_p, E_i being the potential at the foot of the wave, according to equation (11).

$$\log i = K - \frac{\alpha nF}{RT}(E - E_i) \qquad (11)$$

The calculated value, $\alpha = 0.6$ ($\nu = 5000$ mV s^{-1}, $c_L:c_M = 20:1$) has been confirmed by the equation $E_p - E_p = [48/(\alpha n)]$ for the same scan rate with $w_{\frac{1}{2}}^c = -2(E_p^{'} - E_p) = 160$ mV and $n = 1$. The quasi-reversible character of this system is also confirmed by the observation of a cathodic shift of E_p^c (*ca.* 30 mV for a ten-fold increase in scan rate) this being clearer for higher scan rates (for example $\nu = 1000$ and 10 000 mV s^{-1}). Some adsorption is observed at high scan rates. An increase on i_p^a/i_p^c is observed, which rises from *ca.* 0.4 (for $\nu = 300$ mV s^{-1}) to *ca.* 1.0 (for $\nu = 5$ V s^{-1}), this showing an EC mechanism is probably operative during the electrochemical process.

The half-wave potential in this system was observed to become more cathodic with increasing pH up to a limiting value (*ca.* −700 mV *vs.* SCE). For values of pH between 3 and 7 a cathodic shift of E_p^c was observed, at an approximate rate of 80 mV per pH unit (see Fig. 12). This observation is consistent with protonation of the reduced species [the iron(II) complex] and so one proton and one electron are involved in a quasi-reversible process ($\alpha = 0.6$), according to equation (12).

$$[Fe^{III}(HL)]^+ + H^+ + e^- \rightleftharpoons [Fe^{II}(H_2L)]^+ \qquad (12)$$

For $\nu = 2000$ mV s^{-1}, where irreversible chemical dissociation of the reduced complex is practically not detectable, and adsorption not significant, we can calculate the global formation constant for the reduced monoprotonated species [$\beta^{II}_{Fe(H_2L)}$] from equation (13), derived from the DeFord and Hume equation,[32b] considering that, at pH 6.94, $[Fe^{III}(HL)]^+$ and $[Fe^{II}(H_2L)]^+$ are the main iron-(III) and -(II) complex species respectively.

$$E_p^c - E_p^s = \frac{-59.15}{\alpha}\left[\log \frac{\beta^{III}_{Fe(HL)}}{\beta^{II}_{Fe(H_2L)}} + pH\right] \qquad (13)$$

Substituting $E_p^c = -630$ mV, $E_p^s = 479$ mV (as previously defined)[13] and the global formation constant for the oxidized species, corrected for 1 mol dm^{-3} ionic strength [log $\beta^{III}_{Fe(HL)} = 24.2$], we have log $\beta^{II}_{Fe(H_2L)} = 19.9$. The rate constant for the irreversible dissociation of the iron(II) complex was calculated according to our previous study,[14] using a Nicholson and Shain[33] theoretical approach. For scan rates between 200 and 1000 mV a value of $k_d = 0.8 \pm 0.1$ s^{-1} has been calculated (see Table 3).

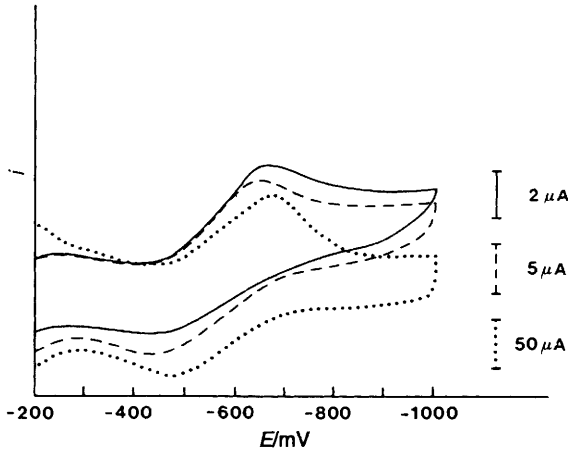

Fig. 11 Cyclic voltammograms for the Fe–H_3L system at pH 7.0 and different scan rates: $\nu = 100$ (——), 1000 (– – –) and 10 000 (• • •) mV s^{-1}; $c_L/c_{Fe} = 20:1$, $c_{Fe} = 5 \times 10^{-4}$ mol dm^{-3}

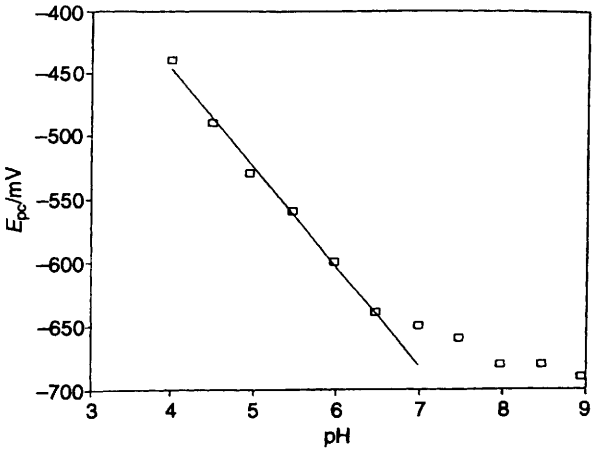

Fig. 12 Cathodic shift of the reduction peak (E_p^c) observed in the cyclic voltammograms of the Fe–H_3L system as a function of pH, at scan rate ν of 1000 mV s^{-1}; $c_L/c_{Fe} = 20:1$, $c_{Fe} = 5 \times 10^{-4}$ mol dm^{-3}

Biological Activity.—Biologically testing establishes that $[Fe(HL)]^+$ functions as a good siderophore in various bacteria, for example in the gram-positive *Anthrobacter flavescens* which generally recognizes all kinds of hydroxamates, and in the gram-negative *Escherichia coli* and *Proteus* strains recognizing hydroxamate, carboxylate and ketohydroxy bidentate siderophores.[16] Further studies for clarifying the mechanism involved in the biological activity are in progress, namely biological assays, to determine the involved outer membrane receptor mediating uptake into the bacterial cells, and kinetics of iron release from the iron(III) complex by edta. However, mainly based on our set of results, some aspects related to the biological role can be speculated on.

The fact that the $[Fe^{II}(H_2L)]^+$ is much less stable than the corresponding oxidized species, together with the observation of its fast probable dissociation (or decomposition), supports the existence of a biological role for this hydroxamate ligand in the metal transport, involving reduction of its iron(III) complex. However the involvement of amine/ammonium ion moieties in recognition of the siderophore analogue complex at the membrane water interface should also be considered as has recently been suggested for aminohydroxamic acids[10] and ferrioxamine B.[39]

The membrane recognition of this siderophore analogue can be speculatively ascribed to the fact that this ligand, having a set of closely separated protonated and unprotonated amine groups (Scheme 4, **a**), becomes able to mimic to some extent the role of ferrichrome amide groups (Scheme 4, **b**), in providing hydrogen-binding interactions with membrane receptors.

Therefore, it can be speculated that these amine groups either have the ability of mimicking the amide group function in membrane recognition, or that they are recognized by differing protein receptors. In this context, a novel outer-membrane receptor protein, involved in ferrioxamine transport, has recently been detected.[40]

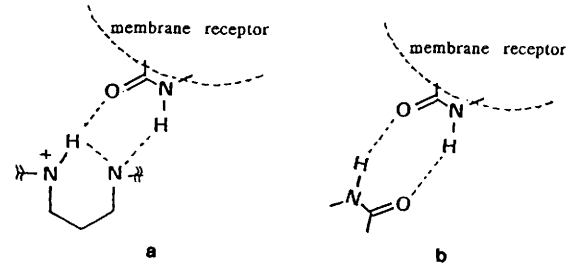

Scheme 4

Table 3 Scan rate effect on the i_p^a/i_p^c ratio and calculated kinetic parameters for the iron(II)–H_3L system at pH 7; $c_L:c_{Cu} = 20:1$, $c_{Fe} = 5 \times 10^{-4}$ mol dm^{-3}

v/mV s^{-1}	i_p^a/i_p^c	$k_d\tau$	$E_{\frac{1}{2}}$/mV	τ^*/s	k_d/s^{-1}
200	0.42	1.52	545	2.28	0.67
300	0.50	0.99	530	1.56	0.63
400	0.55	0.78	530	1.18	0.66
500	0.57	0.72	535	0.93	0.77
600	0.58	0.69	530	0.78	0.88
700	0.59	0.66	530	0.67	0.99
800	0.62	0.57	530	0.59	0.97
900	0.65	0.51	530	0.52	0.98
1000	0.70	0.41	535	0.46	0.89

* See Table 1.

Conclusion

A new biologically active macrocyclic triazatrihydroxamate ligand H_3L has been synthesized. As well as a study of its interaction with protons and copper, special attention has been paid to properties related with iron interaction and siderophore analogy with ferrichrome. Although this ligand presents a slightly lower capability for complexation with iron(III) than does the ferrichrome, the fact that it can be more easily reduced at physiological conditions and that it has a set of closely protonated and unprotonated amino groups could render important biological properties.

Experimental

Synthesis.—Analytical grade reagents were used as supplied and solvents were dried according to standard methods. The macrocycle 1,5,9-triazacyclododecane was synthesized by Richman–Atkins methods.[19,20]

*O-Benzyl-*N*-[(2,2,2-trichloroethoxy)carbonyl]hydroxylamine.* To an ice-cooled suspension of *O*-benzylhydroxylamine hydrochloride (4.00 g, 0.025 mol) and pyridine (4.04 cm^3, 0.050 mol) in dry acetonitrile (50 cm^3) was added dropwise a solution of 2,2,2-trichloroethyl chloroformate (3.38 cm^3, 0.025 mol) in dry acetonitrile (30 cm^3) with stirring under N_2. The reaction mixture was then left at room temperature with stirring under N_2 for 1 h. Volatile components were evaporated under reduced pressure, and the residue was dissolved in ethyl acetate. This solution was washed with 0.5 mol dm^{-3} citric acid, water, 0.6 mol dm^{-3} $NaHCO_3$ and brine and then dried over anhydrous Na_2SO_4. The solvent was evaporated and the product was obtained as a colourless oil (7.19 g, 96%). IR (neat): 1740 cm^{-1} (C=O). ^{1}H NMR ($CDCl_3$): δ 4.80 (s, 2 H, CH_2Ph), 4.93 (s, 2 H, CH_2CCl_3) and 7.39 (m, 5 H, Ph).

*O-Benzyl-*N*-methyl-*N*-[(2,2,2-trichloroethoxy)carbonyl]hydroxylamine.* To a suspension of *O*-benzyl-*N*-[(2,2,2-trichloroethoxy)carbonyl]hydroxylamine (7.20 g, 0.024 mol) and K_2CO_3 (3.33 g, 0.024 mol) in acetone (50 cm^3) was added methyl iodide (2.25 cm^3, 0.036 mol). The reaction mixture was stirred at room temperature overnight. It was filtered and the filtrate evaporated under reduced pressure. The residue was taken up into diethyl ether and washed with water, 0.5 mol dm^{-3} NaOH and brine. The organic phase was then dried over Na_2SO_4 and the solvent evaporated. The product was obtained as a pale yellow oil (6.83 g, 91%). IR (neat): 1730 cm^{-1} (C=O). ^{1}H NMR ($CDCl_3$): δ 3.16 (s, 3 H, CH_3), 4.83 (s, 2 H, CH_2Ph), 4.94 (s, 2 H, CH_2CCl_3) and 7.37–7.39 (m, 5 H, Ph) (Found: C, 42.20; H, 3.90; N, 4.25. Calc. for $C_{11}H_{12}Cl_3NO_3$: C, 42.25; H, 3.85; N, 4.50%).

*O-Benzyl-*N*-methylhydroxylamine.* To a solution of *O*-benzyl-*N*-methyl-*N*-[(2,2,2-trichloroethoxy)carbonyl]-hydr oxylamine (6.50 g, 0.021 mol) in acetic acid (100 cm^3) was added zinc dust (2.72 g, 0.042 mol). The mixture was allowed to stir at room temperature for 30 min. The reaction mixture was then filtered and the filtrate was taken up into ethyl acetate and washed with saturated K_2CO_3 and saturated NaCl. After the extract was dried over Na_2SO_4 and the solvent evaporated, the product was obtained as a colourless oil. To obtain the product as a hydrochloride salt the oil was dissolved in benzene and the solution was then acidified with gaseous HCl. Concentration of the solution under reduced pressure leads to precipitation of the product. Recrystallization of the solid from benzene gave white crystals (1.84 g, 51%), m.p. 89–91 °C (97–99 °C).[41] ^{1}H NMR (D_2O): δ 2.97 (s, 3 H, CH_3), 5.09 (s, 2 H, CH_2Ph) and 7.46 (m, 5 H, Ph).

*O-Benzyl-2-bromo-*N*-methylacetohydroxamic acid.* A suspension of *O*-benzyl-*N*-methylhydroxylamine hydrochloride (1.00 g, 5.80 mmol) and K_2CO_3 (1.76 g, 0.013 mol) in dry tetrahydrofuran (50 cm^3) was cooled in ice with stirring under N_2 for 15 min. Bromoacetyl bromide (1.22 g, 6.1 mmol) in dry tetrahydrofuran (20 cm^3) was then added dropwise over a period of 30 min. After the addition, the reaction mixture was allowed slowly to reach room temperature and left for 7 h with stirring. It was then filtered and the filtrate evaporated under reduced pressure. The residue was dissolved in ethyl acetate and washed with 0.5 mol dm^{-3} citric acid, water, 0.6 mol dm^{-3} $NaHCO_3$ and brine, and dried over anhydrous Na_2SO_4. After evaporation of the solvent the residue was flash chromatographed on a column of silica gel eluting with CH_2Cl_2. The product was obtained as a colourless oil (0.53 g, 36%). IR (neat): 1670 cm^{-1} (C=O). ^{1}H NMR ($CDCl_3$): δ 3.27 (s, 3 H, NCH_3), 3.91 (s, 2 H, $BrCH_2$), 4.94 (s, 2 H, CH_2Ph) and 7.41 (m, 5 H, Ph) (Found: C, 46.55; H, 4.85; N, 5.60. Calc. for $C_{10}H_{12}BrNO_2$: C, 46.55; H, 4.65; N, 5.45%).

*1,5,9-Triazacyclododecane-*N,N′,N″*-tris(O-benzyl-*N*-methylacetohydroxamic acid)* To a suspension of 1,5,9-triazacyclododecane (0.15 g, 0.85 mmol) and NaH (0.07 g, 2.80 mmol) in dry dimethylformamide (dmf) (30 cm^3) was added dropwise a solution of *O*-benzyl-2-bromo-*N*-methylacetohydroxamic acid (0.72 g, 2.80 mmol) in dry dmf (10 cm^3) with stirring under N_2. After the addition, the mixture was stirred at 90–100 °C for 2 h and then for 18 h at room temperature. The mixture was taken up into ethyl acetate (120 cm^3) and washed with concentrated NaCl solution. The organic extract was dried over Na_2SO_4 and after evaporation of the solvent an oil was obtained (0.489 g, 82%) which was directly used in the preparation of H_3L. ^{1}H NMR ($CDCl_3$): δ 1.83 (m, 6 H, NCH_2CH_2), 2.64 (t, 12 H, CH_2NCH_2), 3.12 (s, 9 H, NCH_3), 3.12 (s, 6 H, NCH_2CO), 4.84 (s, 6 H, CH_2Ph) and 7.38 (m, 15 H, Ph).

*1,5,9-Triazacyclododecane-*N,N′,N″*-tris(N-methylacetohydroxamic acid).* The above compound (0.49 g, 0.70 mmol) was dissolved in dry methanol (30 cm^3) and treated with 10% Pd/C (0.18 g) under H_2 (1 atm, *ca.* 1×10^5 Pa) for 4 h at room temperature. The mixture containing the inorganic material was filtered and the solvent was evaporated under reduced pressure. The residue was chromatographed on a column of silica gel eluted with MeOH–CH_2Cl_2 (2:5, v/v). The obtained oil was dissolved in acetone and acidified with gaseous HCl until precipitation of the solid. After filtration and drying under vacuum the product was obtained as a white powder, which was then recrystallized from MeOH and stored under N_2 (0.182 g, 40%). M.p. 120–122 °C. IR(KBr): 1630 cm^{-1} (C=O). ^{1}H NMR (D_2O, pH 1.65): δ 2.17 (m, 6 H, NCH_2CH_2), 3.26 (s, 9 H, NCH_3), 3.31 (t, 12 H, CH_2NCH_2) and 4.11 (s, 6 H, CH_2CO). *m/z* 433 $(M + 1)^+$ and 417 $(M - 16)^+$.

Potentiometric Measurements.—The pH potentiometry titrations were conducted at 25.0 ± 0.1 °C, at an ionic strength of 0.10 mol dm^{-3} (KNO_3) using a Crison Digilab 517 instrument with an Ingold U1330 glass electrode and an Orion 90-00-11 Ag–AgCl reference electrode, with a Wilhelm-type salt bridge containing 0.10 mol dm^{-3} NMe_4NO_3 solution. The calculations of the potentiometric data were performed with the SUPERQUAD program.[42] The purity of the ligand and exact concentrations of the stock solutions were determined by

Gran's method.[43] The electrode calibration was carried out from a titration of a strong acid with a strong base at the same ionic strength. The equilibrium chemical models were selected on the basis of a critical evaluation of the least-squares results and of statistical analysis of the weighted residuals.

Spectrophotometric Measurements.—All spectra were measured on a Lambda 9 Perkin-Elmer spectrophotometer at 25 °C, using 1 cm cells. Solutions of the metal complexes were generated *in situ*, by addition of a standard metal ion nitrate solution to an excess of the ligand. The pH measurements were carried out using a 420 A Orion pH-meter, equipped with an Orion 91-03 glass calomel combination electrode. The stability constants for the iron(III) complex were evaluated from the spectrophotometric titration data using the PSEQUAD computer program.[44] All the spectrophotometric studies were conducted at a constant ionic strength of 0.10 mol dm^{-3} (KNO_3).

Electrochemical Measurements.—Cyclic voltammograms were recorded using a three-electrode system with a hanging mercury drop working electrode, platinum auxiliary electrode, and saturated calomel reference electrode (SCE). All measurements were performed with a Princeton Applied Research PAR 173 instrument coupled with a Nicolet 305 oscilloscope for high scan rates. All solutions were 1.0 mol dm^{-3} in KNO_3, thermostatted at 25 °C and degassed with N_2. The cyclic voltammetric behaviour of copper– and iron–H_nL systems were studied at varying scan rates (v = 200–20 000 mV s^{-1}) and pH. The pH measurements were performed with a 420A Orion pH-meter, equipped with an Orion 91-03 combined electrode.

Other Measurements.—Proton NMR spectra were measured on a Varian Unity 300 spectrometer at 25 °C. Chemical shifts are reported in ppm (δ) from internal references {tetramethylsilane in $CDCl_3$ solutions and sodium 3-(trimethylsilyl)-[2,2,3,3-$^2H_4$]propionate in D_2O solutions}. The following abbreviations were used: s = singlet; d = doublet; t = triplet; m = multiplet. Proton NMR titrations were conducted in D_2O with 2×10^{-2} mol dm^{-3} ligand concentrations. The pD* (operational pD, since the pH meter was standardized with conventional buffers at pH 4 and 7) was varied by adding DCl or KOD (CO_2 free). The final pD* was monitored using a 420A Orion pH-meter fitted with a combined Ingold 6030-02 microelectrode. Melting points were measured on a Buchi 530 capillary apparatus. IR spectra were recorded on a Perkin-Elmer 683 spectrophotometer, and mass spectra were obtained from a modified double-focusing AEI-MS9 spectrometer updated with a VG-Micromass ZAB console and EI/FAB sources. Elemental analyses were done with a Perkin-Elmer 240B elemental analyser.

Acknowledgements

The authors thank Professor J. J. Fraústo da Silva for helpful discussions on the potentiometric results. We also thank Professor G. Winkelmann (Tübingen University), for his collaborative efforts in both carrying out all the biological tests and allowing us to publish some of his previous results. This work was supported by Centro de Química Estrutural-IA (Instituto Superior Técnico) and Junta Nacional de Investigação Cientifica e Tecnológica.

References

1 K. N. Raymond and T. P. Tufano, *The Biological Chemistry of Iron*, eds. H. B. Dolphin, K. N. Raymond and L. Seiker, D. Reidel Publishing Co., Dordrecht, 1982, pp. 85–105.
2 R. R. Crichton, *Inorganic Biochemistry of Iron Metabolism*, Ellis Horwood, Chichester, 1991.
3 C. Carrano, S. R. Cooper and K. N. Raymond, *J. Am. Chem. Soc.*, 1979, **101**, 599.
4 M. S. Mitchell, D. L. Walker, J. Whelan and B. Bosnich, *Inorg. Chem.*, 1987, **26**, 396.
5 I. Dayan, J. Libman, Y. Agi and A. Shanzer, *Inorg. Chem.*, 1993, **32**, 1467.
6 S. Barclay, B. H. Huynn and K. N. Raymond, *Inorg. Chem.*, 1984, **23**, 2011.
7 Y. Sun and A. Martell, *Tetrahedron*, 1990, **46**, 2725.
8 M. Akiyama, A. Katoh and T. Ogawa, *J. Chem. Soc., Dalton Trans.*, 1989, 1213.
9 B. Kurzak, E. Farkas, T. Glowiak and H. Kozlowski, *J. Chem. Soc., Dalton Trans.*, 1991, 163.
10 E. Leporati, *J. Chem. Soc., Dalton Trans.*, 1988, 953.
11 D. A. Brown, M. V. Chidambaram and J. D. Glennon, *Inorg. Chem.*, 1980, **19**, 3260.
12 E. B. Paniago and S. Carvalho, *Inorg. Chim. Acta*, 1987, **136**, 159.
13 M. A. Santos, M. A. Esteves, M. C. T. Vaz and M. L. S. Simões Gonçalves, *J. Chem. Soc., Dalton Trans.*, 1993, 927.
14 M. A. Santos, M. A. Esteves, M. C. T. Vaz and M. L. S. Simões Gonçalves, *Inorg. Chim. Acta*, 1993, **214**, 47.
15 M. A. Santos and M. G. B. Drew, European Research Conference on Chemistry of Metals in Biological Systems, Albufeira, Portugal, 1993.
16 G. Winkelmann, personal communication.
17 J. Leong and J. B. Neilands, *J. Bacteriol.*, 1976, **126**, 823.
18 T. Emery, L. Emery and R. K. Olson, *Biochem. Biophys. Res. Commun.*, 1984, **119**, 1191.
19 J. E. Richman and T. J. J. Atkins, *J. Am. Chem. Soc.*, 1974, **96**, 2268.
20 J. T. Atkins, J. E. Richman and W. F. Oetle, *Org. Synth.*, 1978, **58**, 86.
21 S. Prabhakar, A. M. Lobo and M. A. Santos, *Synthesis*, 1984, 829.
22 B. A. Lee, G. J. Gerfen and N. J. Miller, *J. Org. Chem.*, 1984, **49**, 2418.
23 M. T. Beck and I. Nagypál, *Chemistry of Complex Equilibrium*, Ellis Horwood, Chichester, 1990.
24 J. R. Ascenso, M. A. Santos, J. J. R. Fraústo da Silva, M. C. T. Vaz and M. G. B. Drew, *J. Chem. Soc., Perkin Trans. 2*, 1990, 2211.
25 L. J. Zompa, *Inorg. Chem.*, 1978, **17**, 2531.
26 C. F. G. C. Geraldes, A. D. Sherry, M. P. Marques, M. C. Alpoim and S. Cortes, *Inorg. Chem.*, 1990, **29**, 5.
27 C. Anderegg, F. L. L'Eplattenier and G. Schwarzenbach, *Helv. Chim. Acta*, 1963, **46**, 1409.
28 T. W. Bell, H.-J. Choi and H. Harte, *J. Am. Chem. Soc.*, 1986, **108**, 7427.
29 A. E. Martell and R. M. Smith, *Critical Stability Constants*, Plenum, New York, 1974, vol. I, p. 207.
30 R. Delgado, J. J. R. Fraústo da Silva, M. T. S. Amorim, M. F. Cabral, S. Chaves and J. Costa, *Anal. Chim. Acta*, 1991, **245**, 271.
31 B. Kurzak, L. Nakonieczna, G. Rusek, H. Kozlowski and E. Farkas, *J. Coord. Chem.*, 1993, **28**, 17.
32 (*a*) J. Heyrovsky and J. Kuta, *Principles of Polarography*, Academic Press, New York, 1966, p. 156; (*b*) D. DeFord and D. H. Hume, *J. Am. Chem. Soc.*, 1951, **73**, 532.
33 R. S. Nicholson and I. Shain, *Anal. Chem.*, 1964, **36**, 706.
34 P. Zanello, R. Seeber, A. Cinquantini, G.-A. Mazzocchin and L. Fabbrizzi, *J. Chem. Soc., Dalton Trans.*, 1982, 893.
35 CERIUS program, Version 3.0, Molecular Simulation Inc, Cambridge, 1993.
36 A. K. Rappe, C. J. Casewit, K. S. Colwell, W. A. Goddard, III and W. M. Skiff, *J. Am. Chem. Soc.*, 1992, **114**, 10024.
37 K. N. Raymond and C. J. Carrano, *Acc. Chem. Res.*, 1979, **12**, 183.
38 D. J. Brockway, K. S. Murray and P. J. Newman, *J. Chem. Soc., Dalton Trans.*, 1980, 1112.
39 I. Spasojevic, I. Batinic-Haberle, P. L. Choo and A. L. Crumbliss, *J. Am. Chem. Soc.*, 1994, **116**, 5714.
40 I. Berner, P. Yakirevitch, J. Libman, A. Shanzer and G. Winkelmann, *Biol. Metals*, 1991, **4**, 186.
41 B. J. R. Nicolaus, G. Pagani and E. Testa, *Helv. Chim. Acta*, 1962, **45**, 1382.
42 P. Gans, A. Sabatini and A. Vacca, *J. Chem. Soc., Dalton Trans.*, 1985, 1195.
43 G. Gran, *Acta Chem. Scand.*, 1950, **4**, 599.
44 L. Zekany and I. Nagypal, in *Computational Methods for the Determination of Stability Constants*, ed. D. Legget, Plenum, New York, 1985.

Received 26*th January* 1995; *Paper* 5/00464K